Available online at www.sciencedirect.com

ScienceDirect

Procedia CIRP 13 (2014) 78 – 83

www.elsevier.com/locate/procedia

2nd CIRP 2nd CIRP Conference on Surface Integrity (CSI)

Numerical and experimental analysis of residual stresses generated in the machining of Ti6Al4V titanium alloy

Piotr Niesłony[a]*, Wit Grzesik[a], Piotr Laskowski[b], Jan Sienawski[c]

[a]*Opole Uniwersity of Technology, 5 Mikolajczyka Str., 45-271 Opole, Poland*
[b]*PZL WSK Rzeszów, 120 Hetmańska Str., 35-078 Rzeszów, Poland*
[c]*Rzeszów University of Technology, 12 Powstańców Warszawy Str., 35-959 Rzeszów, Poland*
* Corresponding author. Tel.: +48 77 449 8460.*E-mail address*: p.nieslony@po.opole.pl.

Abstract

This paper presents 2D and 3D FEM simulation results concerning the distribution of residual stresses in the sublayer of machined parts made of Ti6Al4V titanium alloy. FEM simulations were performed for power law and J-C (Johnson-Cook) material constitutive models. Machining tests were carried out using carbide cutting tools coated with a TiAlN monolayer without coolants. The selection of machining conditions was based on real production data. In addition, a real CAD model of the cutting tool insert was implemented. Moreover, an advanced technique of meshing the cutting edge and the grooved rake face was applied. Residual stresses in the machined parts were measured using X-ray diffraction technique. Finally, FEM simulations were compared with measurements in order to recommend the best simulation strategy.

Keywords: finite element method; machining; residual stress

1. Introduction

Residual stresses are often induced in the manufacturing process. The compressive residual stress is beneficial when fatigue strength is being considered and hence is sought after, while the tensile residual stresses should be avoided [1]. This is especially important when machining titanium alloys. The major application of these alloys is in the aerospace industry, where it is used both in airframes and engine components.

Residual stresses significantly affect product performance and serve as a key criterion for process selection, for example in making aerospace engine components. The characterization and prediction of residual stresses for improving product performance has a great economic value [2,3]. Hence, it is also crucial scientific problem [4,5].

The FEM simulations of metal cutting employ several phenomenological plasticity models including mostly Power Law (PL) and Johnson-Cook (J-C) models. The J-C model has been widely used in FEM simulation of metal cutting to predict residual stresses, but this model lacks a mechanism to capture history effect of strain path, strain-rate, and temperature in manufacturing processes [2,6]. Moreover, the influence of machining parameters on the residual stress characteristics is not still properly reflected by FE simulation results. The paper is, in general, focused on the influence of the constitutive models of the workpiece material on the results and simulation accuracy when performing two (2D) and three (3D) dimensional turning operations. In this study a Ti–6Al–4V alloy was machined using TiAlN coated grooved carbide tools.

2. Methodology of investigations

In this study, non-orthogonal turning was carried out on a CNC lathe equipped with Kistler9257B piezoelectric dynamometer with 5019B amplifier and NI 6062E, National Instruments, A/D multi-channel board.

doi:10.1016/j.procir.2014.04.014

The visualization of the recorded force signals and their processing was performed using CutPro data acquisition system. The experimental and simulation conditions are specified in Table 1.

Table 1.Configurations of experimental and numerical simulations

Cutting condition	v_c=80 m/min, a_p=0.125 and 2 mm, f=0.05 and 0.15 mm/rev
Tool data	Grooved tool (KM) type CNMG 120412-UP Sintered carbide insert H10 coated with TiAlN layer of 3 µm thick Cutting edge radius r_n=50 µm
Tool geometry	Cutting tool angles: orthogonal rake γ_0=-5°, orthogonal clearance α_0=5°, back rake γ_p=-4.55°, side rake γ_f=-5.41°, tool inclination angle λ_s=-5.0° Tool nose radius r_ε = 1.2 mm
Constitutive material models	Power Law (PL) Johnson-Cook model (J-C1) Johnson-Cook model with defined thermophysical properties of workpiece material (J-C2)
Simulation models	Two dimensional(2D) Three dimensional (3D)

In these investigations FEM simulations were performed for two fundamental constitutive models including Power Law (set of parameters are shown in Table 2) and Johnson-Cook (J-C) models. The mathematical formulations are presented in [7] and [8] respectively.

Table 2. Johnson–Cook (J-C1) [9] and Power Law (PL) material models parameters for Ti–6Al–4V

Code	A, MPa	B, MPa	n	C	m	$\dot{\varepsilon}_0^p$ 1/s
J-C1	968	380	0.421	0.0197	0.577	1.0
Code	σ_o, MPa	n	ε_0^p	ε_{cut}^p	$\theta(t)$	
PL	952	22.19	0.035	0.12	c_0=1.822 c_1=-0.00571 c_2=1.7 10^{-5} c_3=-2.164 10^{-8} c_4=6.48 10^{-12}	
Melting temperature			1655 °C			
Young modulus			110 GPa			
Poisson ratio			0.3			
Coefficient of thermal expansion			9.4 10^{-6} 1/K			
Density			4430 kg/ m^{-3}			

The J-C model is a well-accepted and numerically robust constitutive material model and highly utilized in modeling and simulation studies. This model assumes that the slope of the flow stress curve is independently affected by strain hardening, strain rate sensitivity and thermal softening behaviors. The J-C model was defined only for a titanium alloy. It should be noted that a range of models with different parameters can be found for Ti–6Al–4V alloy in the literature. For instance, in Table 2 a set of model parameters is specified after Calamaz *et al*. [9], which was coded by J-C1.

Relevant parameters in the PL model were selected from the material data base of AdvantEdge FEM package for a Ti–6Al–4V alloy and the ISO P20 carbide substrate and deposited TiAlN coating.

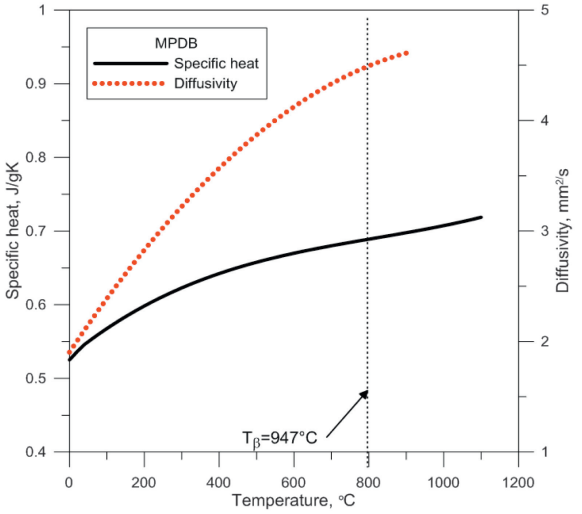

Fig. 1.Specific heat and thermal diffusivity of Ti-6Al-4V versus temperature used in FE simulation [10]

Into the second constitutive J-C model the thermophysical properties of the titanium alloy was implemented using a set of data available in MPDB data base [10]. The changes of the diffusivity and specific heat as a function of temperature are shown in Fig.1 and this part of FE simulations was coded by J-C2.

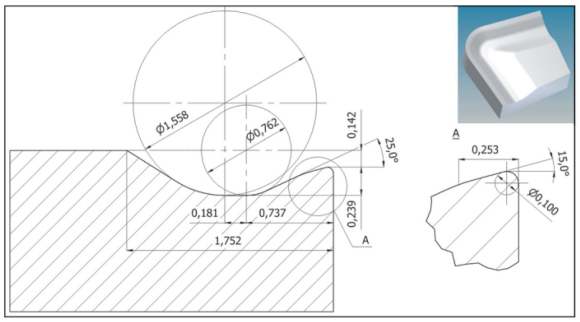

Fig. 2.Dimensioned cross-section of Kennametal cutting insert type CNMG 120412-UP with CAD model of tool edge used in FEM simulation

The experimental set-up and FEM simulations were performed for grooved rake faces. In this case CNMG 120412-UP cutting tool inserts produced by Kennametal were used [11].The measured value of the cutting edge radius for this insert coated by TiAlN monolayer was equal to r_n=50 µm. For the FEM simulation the original 3D CAD model of the grooved cutting insert is used. The dimensioned groove and cutting edge along with magnified corner area are presented in Fig. 2.

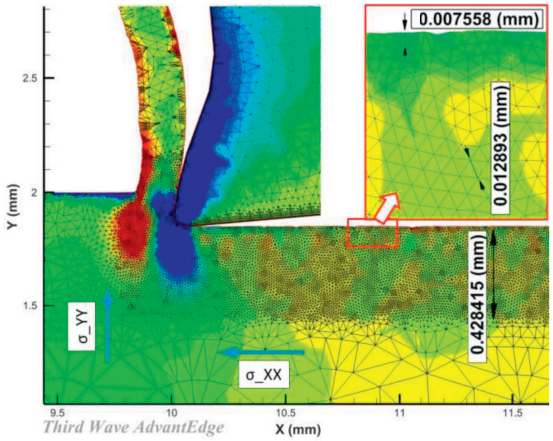

Fig. 3.FEM meshing of the sublayer using special meshing parameters for the designation of stress distribution

In order to predict the stress distribution in the sub layer a special module of AdvantEdge FEM package was used. This allowed the change of meshing parameters in order to obtain a grid of nodes in close proximity (Fig. 3). Average distance of grid nodes in this area was about 7-10 µm, and the thickness of the modified layer was 430 µm.

In this study (Fig.4) the biaxial residual stresses with axial (σ_XX) and tangential (σ_YY) components were measured using the X-ray diffraction method, consisting in the determination of the variations in peak positions due to distortions of the crystalline lattice [12]. The measurements were performed using an iXRDPROTO residual stress measurement system (diffractometer) with portable MG40P standard Ω-2Θ goniometer. The parameters used in the X-ray analysis are shown in Table 3.

Table 3. Parameters used in the X-ray Analysis of Ti–6Al–4V alloy

Test material phase	α-Ti
Spot area, mm^2	4
Wavelengt Radiation	Cu-Kα
Filter	Va
Bragg angle 2Θ, °	138,3 - 143,5(hkl) = (213)
Measuring time, s	20
Changing the detector position, °	0.045

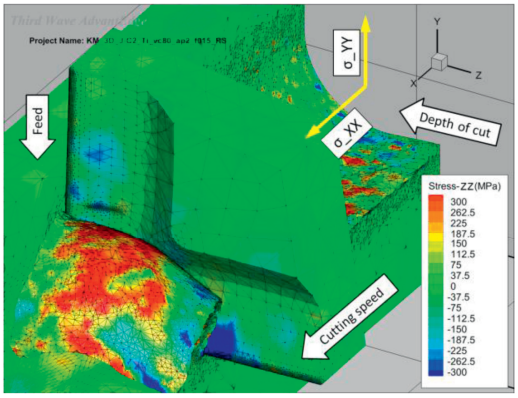

Fig. 4. Layout of the coordinate axes (with residual stresses) and technological parameters used for the 3D FEM modeling

3. Experimental results

The distribution of residual stresses was analyzed in the depth 0.5 mm beneath the surface. Both normal axial σ_XX and tangential σ_YY components were computed. Simulations of these stress components were performed for 2D and 3D machining models with varying feed rate and constant depth of cut and cutting speed of v_c=80 m/min.

FEM simulations were performed using the PL and J-C material constitutive models but in the second case it was modified by implementing the temperature dependent- thermophysical properties of the machined titanium alloy (variant J-C2). It was observed that the form of the constitutive model does not influence the distribution of the residual stress and this fact concerns both 2D and 3D cutting models. It can be seen in appropriate diagrams (Figs. 5-10) that the values of stress decrease to the minimum when the distance from the surface increases (the hook-type distribution of RS is typically determined). After this point, stresses increase and reached the maximum positive value not higher that 200 MPa. At a distance between 0.2-0.5 mm the stresses do not exist. It was found that the depth of cut practically does not influence the distribution and values of RS but, on the other hand, the decisive variable factor is the feed rate.

In general, the increase of the σ_XX and σ_YY stress components in the depth up to 15 µm corresponds to higher feed rate of about f=0.15 mm/rev. For a 3D FEM simulation and a_p =2 mm it was in the range of 150–300 MPa. Moreover, the kind of constitutive model can be neglected in these specific simulations.

In particular, for the PL model (Figs. 5 and 6) the increase of σ_XX and σ_YY was equal to 280 MPa and 100 MPa respectively. In comparison, for the two variants of the J-C model (J-C1 and J-C2) the changes of

stresses were equal to 150-280 MPa and 70-190 MPa depending on the machining conditions applied.

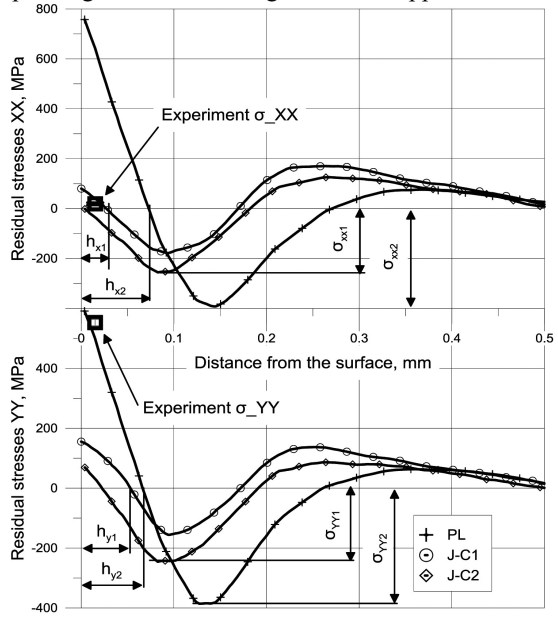

Fig. 5.Distributions of residual stresses in the sub layer obtained for experimental (f=0.15 mm/rev and a_p=2 mm) and 3D FE results

It can be reasoned based on stress distributions shown in Figs. 5-8 that the most intensive changes were obtained for the PL model, when performing 3D simulations. For this case, the maximum differences of RS values in the sublayer were determined.

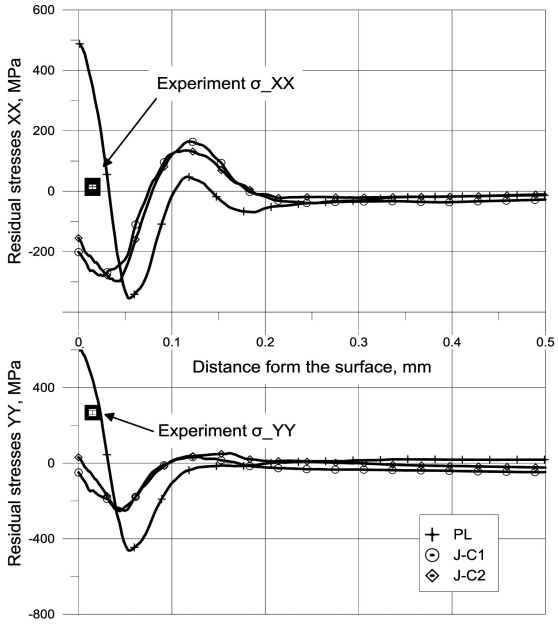

Fig. 6.Distributions of residual stresses in the sublayer obtained for experimental (f=0.05 mm/rev and a_p=2 mm) and 3D FE results

Table 4. Comparison of measured values of residual stress components at different cutting conditions for v_c=80 m/min (σ_XX – axial; σ_YY – tangential stress components)

Depth of cut	Feed rate	σ_XX	σ_YY
mm	mm/rev	MPa	MPa
0.125	0.05	-27±7	407±11
0.125	0.15	-15±4	455±5
2.0	0.05	10±6	268±10
2.0	0.15	19±5	553±10

Due to technical reasons, comparative measurements of the normal axial and tangential stresses concern only the selected points localized at the distance of about 15 µm from the surface. According to the data specified in Table 4 the measured values of tangential tensile RS change in the range of 258 do 563 MPa.

In contrast, the values of axial RS changed in the narrower range from -34 to 24 MPa. Hence, the values of σ_XX stresses are more than 20 times lower than σ_YY stresses. It should be noted that compressive σ_XX stresses were obtained for small feed and close to the surface.

It can be reasoned that the best agreement between predicted and measured σ_YY RS was achieved for the 3D cutting and PL constitutive models (Figs. 5-8). In the case of σ_XX RS this evidence is related to the J-C, and as shown in Fig. 7, independently of its variant (J-C1 and J-C2).

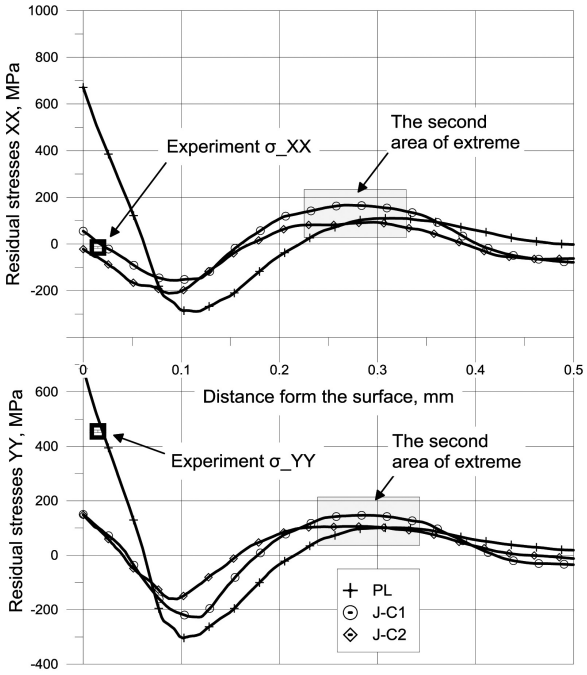

Fig. 7.Distributions of residual stresses in the sublayer obtained for experimental (f=0.15 mm/rev and a_p=0.125 mm) and 3D FE results

The above-mentioned fact can be explained in terms of the thermal softening which is considered in the PL model. In this model, a multi-regressive mathematical model of higher order is used to fit the predicted and measured data. It is obviously known that titanium machining under dry conditions is associated with intensive heat generation and the thermal softening effect can cause that the RS decreases. The final result is that the predicted axial RS are close to the measured values.

It seems, based on the latter hypothesis that the generation of tangential σ_YY stresses is based on the different mechanism. In particular, the decisive factor can be the cutting edge radius. As has been suggested in many literature sources, for instance by Pawade *et al.* [13], machining with more blunter tools (higher cutting edge radius r_n) can result in the increase of tangential RS and the width of the stressed zone.

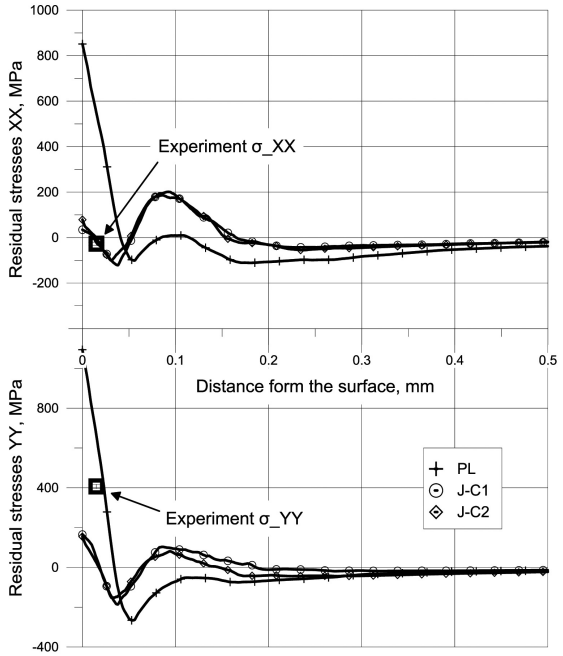

Fig. 8.Distributions of residual stresses in the sublayer obtained for experimental (f=0.05 mm/rev and a_p=0.125 mm) and 3D FE results

It was observed during FEM simulations that the type of material constitutive model is a decisive factor influencing the depth of the zone with induced tensile stresses. Distinctly thicker stressed zone is predicted using the PL constitutive model, as for instance those shown in Fig.5 –depths h_{x2} and h_{y2}. However, values of compressive stresses for this case study are higher than for both J-C1 and J-C2 models (comparison stresses σ_{XX2} and σ_{XX1} , and σ_{YY2} and σ_{YY1} in Fig. 5). This difference can be caused by low diffusivity and low specific heat, as depicted earlier in Fig. 2, when the thin sublayer is intensively heated during cutting. Due to limited heat transfer into the machined material the heat affected zone is very thin. After the cooling, material in this zone shrinks and the compressive RS are generated. The differences in the distribution of RS can also result from accurate modeling of the strain rate effect.

The J-C model assumes that the flow stress is a unique function of the total strain, strain-rate, and temperature, and their effects on the flow stress are independent. On the other hand, this function in the PL model is similar but additionally two sub-regions of $\dot{\varepsilon}_p$ with low and high strain rates are distinguished. The $\dot{\varepsilon}_t$ is the strain rate where the transition between low and high strain rate sensitivity occurs and m^1 and m^2 are the strain rate sensitivity coefficients.

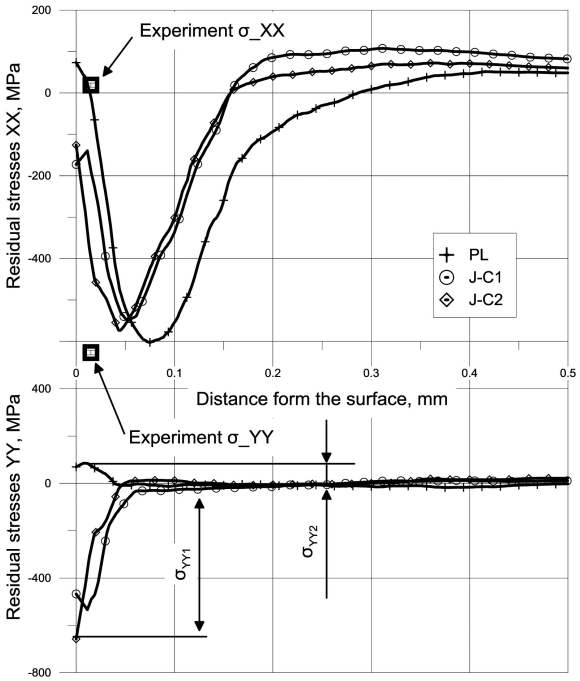

Fig. 9.Distributions of residual stresses in the sublayer obtained for experimental (f=0.15 mm/rev and a_p=2 mm) and 2D FE results

The distributions of RS obtained for the 2D simulations of a Ti-6Al-4V alloy with depth of cut of a_p=2mm and two feed rates of 0.15 and 0.05 mm/rev are shown in Figs. 9 and 10 respectively. It is evident from Figs. 9 and 10 that the feed rate does not influence the distribution of RS in both axial (XX) and tangential (YY) directions. In addition, the shapes of RS distribution differ from those obtained for 3D cutting models, as shown exemplarily in Fig. 7.

In the thin layer adjacent to the surface the compressive σ_XX and σ_YY stresses are produced, although axial stresses are relatively small. Their maximum values (σYY1) were obtained for J-C1 and

J-C2 constitutive material models as illustrated in Figs. 9 and 10.

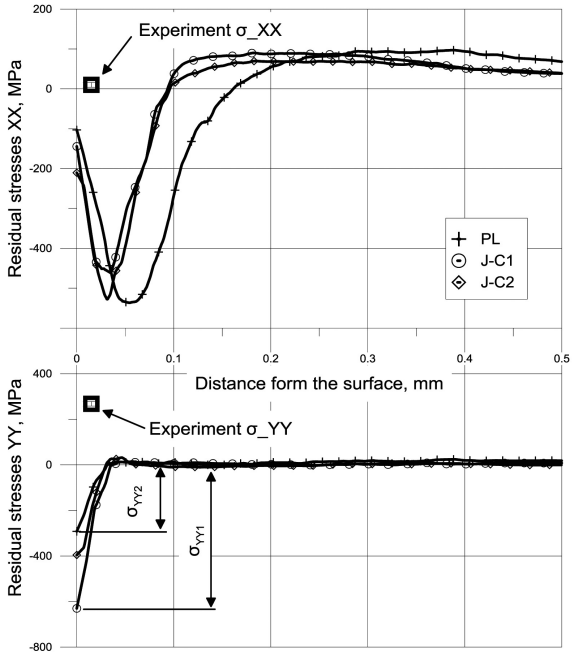

Fig. 10.Distributions of residual stresses in the sublayer obtained for experimental (f=0.05 mm/rev and a_p=2 mm) and 2D FE results

In addition these values are higher than those predicted by the 3D simulations. As a result, the predicted results do not coincide with measurements. It should then be noted that simplified 2D FEM simulations, in which the effect of the roundness of the cutting edge is neglected, cannot be applied in the prediction of RS.

4. CONCLUSION

Based on the experimental results and FEM predictions the conclusions are as follows:

- Prediction of RS in titanium machining depends on the constitutive material model used. In this study, the PL model induces more distinct changes in the RS distribution.
- Additional consideration of the thermo-physical properties of the machined titanium alloy does not change the shape of RS distribution.
- For 3D FEM simulations an acceptable agreement between predicted and measured results was found for the axial stresses σ_XX when using the J-C model and for the tangential stresses σ_YY when using the PL model.
- It was found that the feed rate influences strongly the RS in the technological sublayer. In contrast, the effect of the depth of cut, especially in a 2D simulation can be ignored.
- The shapes of RS distributions obtained by 2D and 3D FEM simulations are different. It can be concluded, based on the selected measurements, that 3D predictions are closer to the XRD data.
- From the practical point of view, 2D FEM simulations of RS in titanium machining using “sharp” tools cannot be recommended. They should be based on the real cutting tool model with defined value of the cutting edge radius.

Acknowledgements

This investigations have been carried out as part of a project No. PBS1-178595 funded by the Polish National Center for Research and Development (NCBiR).

References

[1] Yang X., Liu C.R., 1999. Machining Titanium and Its Alloys. Machining Science and Technology 3/1, p. 107.
[2] Guo, Y.B., Li, W., Jawahir, I.S., 2009. Surface Integrity Characterization and Prediction in Machining of Hardened and Difficult-To-Machine Alloys: A State-of-art Research Review and Analysis. Machining Science and Technology, 13/4, p. 437.
[3] Berruti T., Lavella M., Gola M. M, 2009. Residual Stresses on Inconel 718 Turbine Shaft Samples after Turning. Machining Science and Technology 13/4, p. 543.
[4] Jawahir I. S., Brinksmeier E., M'Saoubi R., Aspinwall D. K., Outeiro J. C., Meyer D., Umbrello D., Jayal A. D., 2011. Surface integrity in material removal processes: Recent advances, Cirp Annals-manufacturing Technology 60/2, p.603.
[5] Outeiro J. C., 2013. Three-dimensional modeling of residual stresses induced by machining plain carbon steel. International Journal of Advanced in Machining and Forming Operations 5/1, p.11.
[6] Ulutan D., Ozel T., 2011. Machining induced surface integrity in titanium and nickel alloys: A review. International Journal of Machine Tools and Manufacture 51, p. 250.
[7] Niesłony P., Grzesik W., Laskowski P., Habrat W., 2013. FEM-Based Modelling of the Influence of Thermophysical Properties of Work and Cutting Tool Materials on the Process Performance. Procedia CIRP 8, p. 3.
[8] Niesłony P., Grzesik W., Chudy R., Laskowski P., Habrat W., 2013. 3D FEM simulation of titanium machining. International Conference on Advanced Manufacturing Engineering and Technologies - NEWTECH 2013, p. 31.
[9] Calamaz M., Coupard D., Girot F., 2008. A new material model for 2D numerical simulation of serrated chip formation when machining titanium alloy Ti–6Al–4V. International Journal of Machine Tools and Manufacture 48, p. 275.
[10] Material Properties Database, MPDB v. 7.51, 2013. JAHM Software, Inc.
[11] Kennametal 2013, May 15. Available: http://www.kennametal.com.
[12] Lu J., 1996 Handbook of measurement of residual stresses. The Fairmont Press Inc.
[13] Pawade R.S., Joshi S.S., Brahmankar P.K., 2008. Effect of machining parameters and cutting edge geometry on surface integrity of high-speed turned Inconel 718. International Journal of Machine Tools and Manufacture 48/1, p. 15.